The quadruple system ADS 1652

A. Tokovinin,[1]★ N. A. Gorynya[2,3] and N. I. Morrell[4]

[1]*Cerro Tololo Inter-American Observatory, Casilla 603, La Serena, Chile*
[2]*Institute of Astronomy of Russian Academy of Science, 48 Pyatnitskaya Str, 109017 Moscow, Russia*
[3]*Lomonosov Moscow State University, Sternberg State Astronomical Institute, Universitetskij prospekt, 13 Moscow 119991, Russia*
[4]*Las Campanas Observatory, Carnegie Observatories, Casilla 601, La Serena, Chile*

ABSTRACT

A detailed study of the rare nearby quadruple system with a three-tier hierarchy is presented, contributing to the still scarce data on such multiples. We compute the first combined spectroscopic and interferometric orbit of HD 12889 with a period of 2.58 yr and eccentricity 0.77. This refers to the inner pair Aa, Ab in the quadruple system ADS 1652 which also contains the visual binary A, B with a known orbit of ∼200 yr period and another companion, C (HD 12873), at a projected distance of 2500 au from A. Photometry of all components is provided. The multiple system is located at a distance of 44 pc and it is composed of main-sequence dwarfs with estimated masses of 0.74, 0.72, 0.57, and 0.78 solar masses for Aa, Ab, B and C, respectively. The orbits of Aa, Ab and A, B are likely coplanar.

Key words: binaries: spectroscopic – binaries: visual – stars: individual: HD 12889.

1 INTRODUCTION

A large fraction of stars belong to binary and multiple systems. Understanding their formation mechanisms and developing a theory capable of explaining and predicting statistical properties of stellar systems is one of the yet unsolved problems in star formation. From this perspective, hierarchical multiples with three or more components are particularly useful because their additional parameters like period ratios and relative orbit orientation constrain the formation scenarios even more than just the binary statistics. Outcomes of large-scale hydrodynamic simulations of star formation (Bate 2012) or numerical simulations of *N*-body dynamics (Reipurth & Mikkola 2012) are to be compared to the solid observational data.

Observational data on multiple systems are hard to get, however, because binary periods and separations span a huge range. The combination of different observing techniques and individual object-by-object approach are needed, meaning that the progress is slow. Reasonable completeness can be reached only in the nearby volume for solar-type primaries. Still, even the best-studied 25-pc sample of Raghavan et al. (2010) has systems with uncertain status or without orbital solutions. Among their 454 targets, there are only three multiple systems with a three-tier hierarchy like the one studied here. The less complete sample of 4847 solar-type stars within 67 pc of the Sun (Tokovinin 2014) contains 21 multiples with three-tier hierarchy; their estimated frequency is about 1 per cent. So, each new well-studied multiple is a non-negligible increment.

We study here a nearby (at 44 pc) system of four low-mass stars. The inner pair Aa, Ab with a period of 2.6 yr and nearly equal components is orbited by the less-massive star B with a period of the order of 200 yr. The most massive component C is located at a projected distance of 2500 au from AB; it is single, as far as we can tell. Why are the two objects that formed together in close proximity so different, one single and another triple? By studying the architecture and dynamics of multiple systems like this one, we gather information that will help to understand eventually their formation and to answer this question.

The multiple system is designated WDS J02057−2423 and is also known as ADS 1652 (Aitken 1932). Its two bright components A and C have separate HD and HIP identifiers and individual entries in SIMBAD, from which the data of Table 1 were gathered. The stars A and C share common proper motion and are located at the same distance. Considering that the *Hipparcos* parallax of A could be affected by its multiplicity, we adopt the parallax of 22.8 mas in the following.

The multiplicity of ADS 1652 was revealed 'from outside in', starting with the 56 arcsec pair AB, C first measured in 1897 (Boss 1918); its relative position remains constant since then. The subsystem A, B was discovered in 1909 by Innes (1912) and received the designation I 454. The binary nature of A was discovered in 1995 by its double lines, while observing it in Crimea with the correlation radial-velocity meter (RVM). During the following 10 yr, double lines were seen on odd years but the object appeared as single-lined on even years. This suggested a 2-yr period, but no orbit could be determined with the limited seasonal coverage from Crimea, restricted by the southern declination of −24°. Tokovinin & Smekhov (2002) simply reported the double-lined observations.

★ E-mail: atokovinin@ctio.noao.edu

Table 1. Basic parameters of ADS 1652.

Comp.	HD	HIP	Spectral type	PM (mas yr^{-1})	π_{HIP2} (mas)
AB	12889	9774	K1V	+418,−57	21.44 ± 1.43
C	12873	9769	G8/K0V	+412,−57	22.81 ± 1.27

The first orbit is published here 19 yr after the discovery of Aa, Ab. Observations at Mt Wilson in the 1920s (Abt 1970) detected the radial velocity (RV) difference between components AB and C, but failed to recognize the double-lined nature of A.

In this paper, we publish the first spectro-interferometric orbit of the sub-system Aa, Ab derived from all available data. The visual orbit of the A, B system, recently computed by Hartkopf, Tokovinin & Mason (2012), is slightly revised. Then, the masses and magnitudes of all components are estimated. The system as a whole and its possible origin are discussed in the last section.

2 OBSERVATIONS

2.1 Correlation RVs

The components A and C were observed in 1995–2007 with the CORAVEL-type instrument, RVM (Tokovinin 1987) at the 1-m telescope of the Simeiz observatory in Crimea. In this instrument, the echelle spectrum is transmitted through a mask with slits corresponding to the spectral lines. The curve of transmitted flux versus relative shift between spectrum and mask represents the cross-correlation function (CCF) between the stellar spectrum and the mask. The range of the CCF, defined by the scanning mechanism of the RVM, is 50 km s^{-1}. The instrumental stability is monitored with a neon lamp, the velocity zero-point is established by observations of several IAU standards each night. The RVs are determined by fitting the CCF by one or two Gaussian functions. More information on this method can be found in Tokovinin & Gorynya (2001).

Owing to the low declination, the object could be observed from Crimea only during observing runs in September–October. Most observations were obtained by NAG. In 2005, the approach to periastron was captured, with the RV difference between Aa and Ab decreasing substantially during one month.

Fig. 1 shows typical CCFs of the A component measured with the RVM and the fitted double Gaussians. To record the full curve, the centre of the 50 km s^{-1} scanning range was set on each component separately, and the two resulting CCFs were stitched together during the fit. The overall trend of the 'continuum' (of instrumental origin) is included in the fitted model. The ratio of the correlation dip surface measured with the RVM leads to Δm(Aa, Ab) = 0.3 mag.

Although the RVM can achieve RV accuracy of 0.3 km s^{-1} on bright RV standards, fits to the noisy and low-contrast CCFs like those in Fig. 1 are much less accurate and can contain systematic errors, aggravated by the low elevation of the star as seen from Crimea.

2.2 RVs from the echelle spectra

NM obtained several spectra at the Las Campanas Observatory (LCO) using the échelle spectrometer at the 2.5-m du Pont telescope. After the first observation on 2007 January 2 (JD 245 4102.524), R. Gamen and G. Preston took another two spectra in 2007 June and July. In January, the lines were unresolved (of the same width as in the C component), while in June and July, the lines of the A
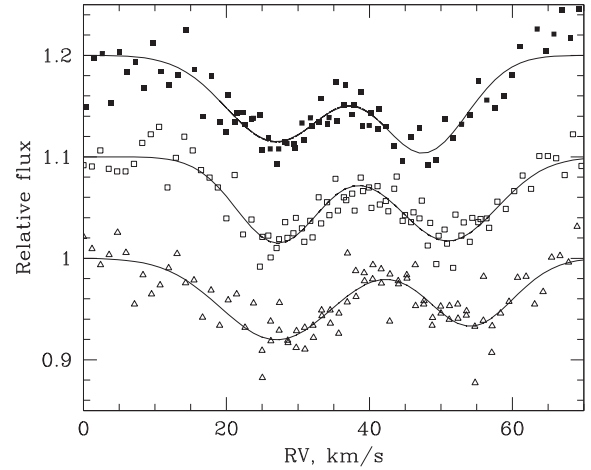

Figure 1. Correlation traces of ADS 1652A observed with the RVM in 1995, 1997 and 2005 (JD 244 9991, 507 09 and 536 13, respectively, top to bottom) displaced vertically by 0.1 for clarity (the horizontal shifts are arbitrary).

component were wider. Another double-lined spectrum was taken on 2007 August 30 by R. Covarrubias with higher resolution using the Mike echelle spectrograph at the Magellan-II Clay telescope, during engineering time.

The echelle spectra taken at LCO with the du Pont and Clay telescopes were processed by the standard IRAF echelle package. The wavelength scale is calibrated by the thorium–argon lamp observed immediately after the star. The polynomial coefficients of the wavelength solution are written into the FITS headers, following the IRAF multispectral format. The wavelength of each pixel was computed from these polynomials with the help of the GETCHELLE.PRO IDL program.[1] The spectra cover wavelengths from 3500 to 9000 Å.

The monitoring at LCO enabled us to finally guess the true orbital period of 2.6 yr. The tentative orbit predicted the periastron passage to occur in 2008 May–June. This episode was actually observed at Cerro Tololo, using the newly assembled fibre echelle spectrometer (FECH) at the 1.5-m telescope. It was the de-commissioned echelle spectrometer from the 4-m Blanco telescope, transferred into the coudé room of the 1.5-m. The detector was a 2K SIT CCD with the Arcon controller. The light was fed from the telescope through a multimode fibre. The object was barely visible above the morning horizon at the time of these observations, but, fortunately, the periastron was not missed. These data are published here for the first time.

The spectra taken with FECH were processed at Yale University by D. Fischer, using an adaptation of the REDUCE package (Piskunov & Valenti 2002) under IDL. The wavelength of each pixel determined from the thorium–argon lamp is written in the FITS file together with the extracted spectrum.

We determined the RVs by digital correlation of spectra with the numerical mask. The mask is binary, it equals one within spectral lines and zero otherwise. This method, successfully used by the Geneva team (Baranne et al. 1996), is a good way to extract the RV information, mostly contained in the 'shoulders' of spectral lines, and a direct numerical analogue of the physical mask in RVM. The mask is constructed from the solar digital spectrum[2] (see also

---

[1] C. Allende Prieto, http://hebe.as.utexas.edu/stools/pros/getchelle.pro
[2] Hinkle, K., Wallace, L., Valenti, J., and Harmer, D. Visible and Near Infrared Atlas of the Arcturus Spectrum, 3727–9300 Å.

Hinkle, Wallace & Livingston 1995). The solar spectrum is normalized by the continuum, so for all its pixels with values less than 0.6, the mask is set to 1 ('slit'). The mask use only the wavelength region from 4500 to 6500 Å, with the spectrum re-binned logarithmically with a step corresponding to 1 km s^{-1} velocity. Slits wider than 10 km s^{-1} are removed from the mask, the remaining 758 slits have a median width of 5 km s^{-1}.

The CCF is computed for each echelle order. A sub-region of the mask corresponding to the wavelength range of the order is selected (omitting 200 points at both ends to allow for the shifts). Then, the order is re-binned on the wavelength scale of the mask, and the CCF is calculated as a product between the spectrum and the shifted mask, with shifts ranging from -200 to $+200$ km s^{-1}. The CCFs of all orders are summed together and normalized by the median CCF (the 'continuum' of the CCF thus equals 1).

The CCFs of single and binary stars are modelled by sums of Gaussian curves. The CCF values above a certain threshold (usually above 0.98) are excluded from the fit, the model has a fixed continuum level of 1. Fig. 2 shows two examples of such fits. This method of RV measurement uses the solar spectrum as a reference and does not rely on any RV standards. The RVs derived in this way might contain a systematic error caused by a subtle difference between the lamp and stellar spectra, but such potential biases are ignored here.
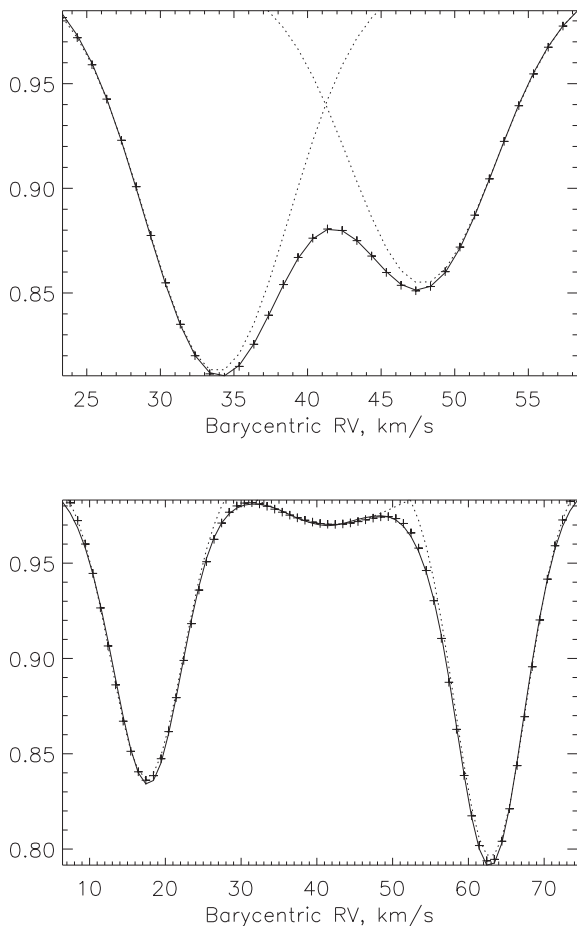

Figure 2. CCFs and their fits by Gaussians. The CCF curves are traced in full lines, the fits are overplotted as crosses, and the individual Gaussians are shown by dotted lines. Top: data from Mike on 2007 August 30 and the two-component fit. Bottom: data of 2008 May 29 from FECH and the three-component fit.

Table 2. Parameters of the CCF fits from the FECH observations in 2008.

Comp.	RV (km s^{-1})	FWHM (km s^{-1})	Amplitude
Aa	var	11.12	0.207
Ab	var	11.38	0.164
B	41.93	20.39	0.034
C	41.05	11.14	0.381

Table 3. RVs of components C and B.

JD +240 0000	RV (km s^{-1})	Err	In.	JD +240 0000	RV (km s^{-1})	Err	In.
	C = HD12873			536 31.539	41.65	0.48	R
499 89.462	40.40	0.32	R	539 72.591	40.52	0.36	R
499 97.485	40.30	0.34	R	539 81.582	40.95	0.53	R
500 03.462	39.63	0.23	R	539 86.555	40.62	0.33	R
503 24.526	40.88	0.47	R	539 91.575	40.29	0.37	R
507 09.561	42.08	0.49	R	543 42.806	40.26	0.10	M
510 55.570	41.01	0.55	R	541 03.519	40.67	0.10	L
510 84.541	39.36	0.47	R	546 16.929	41.05	0.10	F
510 92.492	39.51	0.29	R	546 30.930	40.95	0.10	F
514 42.543	39.53	0.29	R	546 31.919	41.01	0.10	F
522 17.393	39.39	0.46	R		HD 12889B		
532 50.547	41.76	0.39	R	546 15.922	42.205	0.50	F
532 85.487	38.31	1.67	R	546 16.921	41.858	0.50	F
532 85.487	39.15	0.83	R	546 17.914	42.530	0.50	F
536 13.603	42.60	0.92	R	546 23.908	41.270	0.50	F
536 21.607	40.81	0.69	R	546 30.916	41.904	0.50	F
536 28.553	40.79	0.57	R	546 31.911	41.816	0.50	F

Instruments: R – RVM; L – echelle at 100-inch du Pont; M – Mike at Magellan Clay; F – fibre echelle at CTIO 1.5 m.

In 2008 May–June, during maximum velocity separation between Aa and Ab, the CCFs clearly show three components, with the spectrum of B seen between the lines of Aa and Ab (Fig. 2, bottom). These CCFs are fitted by three Gaussians. On the other hand, the CCFs of the component C are fitted by a single Gaussian. Average parameters of the fitted models (RV, full width at half-maximum, FWHM, and amplitude) are listed in Table 2, as determined from six FECH spectra of AB and three spectra of C. The rms scatter of the apparently constant RVs of B and C is 0.42 and 0.05 km s^{-1}, respectively. Table 3 lists the RVs of components C and B measured with the RVM and from the echelle spectra. The weighted rms scatter of 21 RVM velocities of C is 0.84 km s^{-1}, larger than expected from the formal errors listed in the third column of Table 3.

We attempted to extract the spectrum of the B component by fitting the spectrum of A with two suitably shifted and scaled spectra of the single component C. However, this did not produce convincing results because C is hotter than either Aa or Ab and their spectra do not match very well. The difference between the spectrum and its two-component fit, which presumably contains the spectrum of B, is contaminated by the residuals; its cross-correlation with the solar mask shows the narrow dip corresponding to B together with the artefacts in place of Aa and Ab. The width of the dip of B is about 11 km s^{-1}, so this component is not a rapid rotator, and the increased width of its dip reported in Table 2 is not real (the CCFs differ from Gaussian curves in the wings, affecting the weak lines of B). The mismatch between the CCF (line) and its model (crosses) is seen in Fig. 2 (bottom).
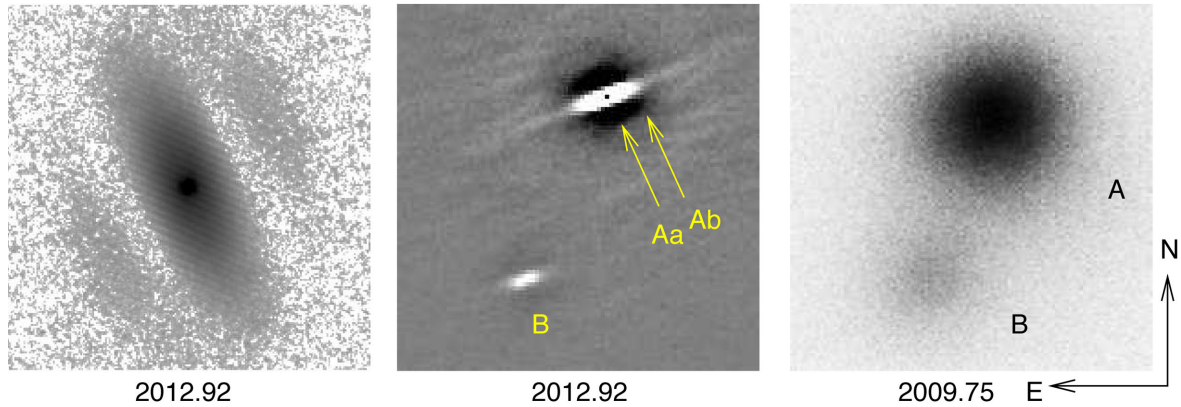
Figure 3. Speckle observations in the *y* band on 2012.92, at maximum separation of Aa, Ab: the power spectrum (left) and the fragment of the ACF with components marked (centre). The right-hand panel shows the direct image in the *I* band recorded on 2009.75 with partial adaptive correction (FWHM resolution 0.47 arcsec, separation 0.80 arcsec).

2.3 Speckle interferometry

The period of 2.6 yr corresponds to the orbital semimajor axis of 47 mas, meaning that the inner pair should be resolvable by speckle interferometry. Indeed, it was marginally resolved at the 4-m Blanco telescope in 2008 July, only two months after passing through the periastron (Tokovinin et al. 2010b). The 'new' pair Aa, Ab was designated as WSI 71. Further speckle monitoring at the 4.1-m SOAR telescope during the following 5.5 yr (Hartkopf et al. 2012; Tokovinin 2012) added several spatial resolutions and non-resolutions of Aa, Ab and new measurements of A, B. Known spectroscopic elements allowed us to derive a preliminary visual orbit of Aa, Ab which was reported by Tokovinin et al. (2010a) in advance of the full analysis presented here.

The equipment used for speckle interferometry and the method of data processing are covered in Tokovinin et al. (2010b). Series of short-exposure images with fine spatial sampling are recorded by an electron-multiplication CCD. The average square modulus of the Fourier transform of all images (power spectrum) is computed and fitted to a model. Fig. 3 shows the power spectrum and the auto-correlation function (ACF) of the triple system (Aa, Ab, B) observed in 2012.9, when the inner pair was near its maximum separation. The peak of B is clearly doubled by its correlation with the pair Aa, Ab. The outer pair A, B can be also resolved directly (without speckle) under very good seeing. In 2009, the object was observed with partial adaptive optics correction (Tokovinin et al. 2010a), and the AB pair was clearly separated in the average re-centred image. The measurement on 2012.92 is published in Tokovinin, Mason & Hartkopf (2014), the last speckle observation of A, B in 2014 January is yet unpublished (the inner pair was unresolved).

The separation of the inner pair Aa, Ab is comparable to or below the diffraction limit of the 4-m telescopes ($\lambda/D = 27$ mas at 540 nm). In such case, the power spectrum has only one 'fringe'. Its width and orientation determine the fitted separation ρ and position angle θ, respectively. However, the width of the fringe also depends on the magnitude difference Δm. Strong correlation between ρ and Δm degrades the un-constrained fits. Moreover, instrumental elongation of the power spectrum caused by telescope vibration or by poorly corrected atmospheric dispersion directly influences the measurements, whereas at larger separations several fringes are present and the instrumental distortion of the power spectrum is effectively de-coupled from the binary parameters.

The published speckle observations of the pairs Aa, Ab and Aa, B are derived by fitting a triple-star model to the observed power spectrum. The parameters of the Aa, Ab pair are strongly affected by the cross-talk between ρ and Δm. Here, we re-processed the speckle data by fitting a simple binary-star model with fixed $\Delta m = 0.2$; the presence of B was ignored. This re-processing improves the internal consistency of the speckle measurements (on each date, the object was recorded at least twice), so we use the re-processed measurements of Aa, Ab in the orbit calculation. However, systematic errors caused by the telescope vibrations can still be present. The measurements on 2008.5 and 2008.7 when Aa, Ab was closer than the diffraction limit are uncertain. On 2009.7, the observation were made in the *I* filter (770 nm), so the Aa, Ab pair was again under the diffraction limit. Only the measurement on 2012.92, at maximum separation, is quite secure because the power spectrum shows the second fringe. We re-examined the data of 2010.96 and 2014.05 to confirm that Aa, Ab was not resolved on those dates and the power spectrum did not show any measurable asymmetry.

3 THE ORBIT OF Aa, Ab

The elements of the combined spectro-interferometric orbit of Aa, Ab and their errors are given in Table 4. They were fitted by the standard least squares with weights inversely proportional to the measurement errors. RVs and speckle measurements are fitted jointly to a common set of orbital elements (Morbey 1992). Uncertain speckle measurements in 2008 (under the diffraction limit) are given low weight by increasing their errors to 10 mas. The measurements in the *I* filter are given errors of 5 mas. The weighted rms residuals are 2°.8 and 1.7 mas in θ and ρ, respectively. The velocity rms residuals for the primary and secondary are 0.46 and 0.44 km s^{-1}, respectively.

Fig. 4 depicts the orbit and the data points. RVs derived from the blended lines (orbital phase from 0.2 to 0.6) are not used in the solution (their errors are increased by 30 km s^{-1}). The RVs of Aa and Ab, their assumed errors, and residuals to the orbit are given in Table 5. The RVs of Ab are missing when the lines were not resolved (blended); the corresponding 'blended' RVs of Aa are given artificially large errors. The speckle measurements and their residuals are found in Table 6. The computed position is given in brackets in place of residuals when the binary was not resolved.

Table 4. Orbital elements.

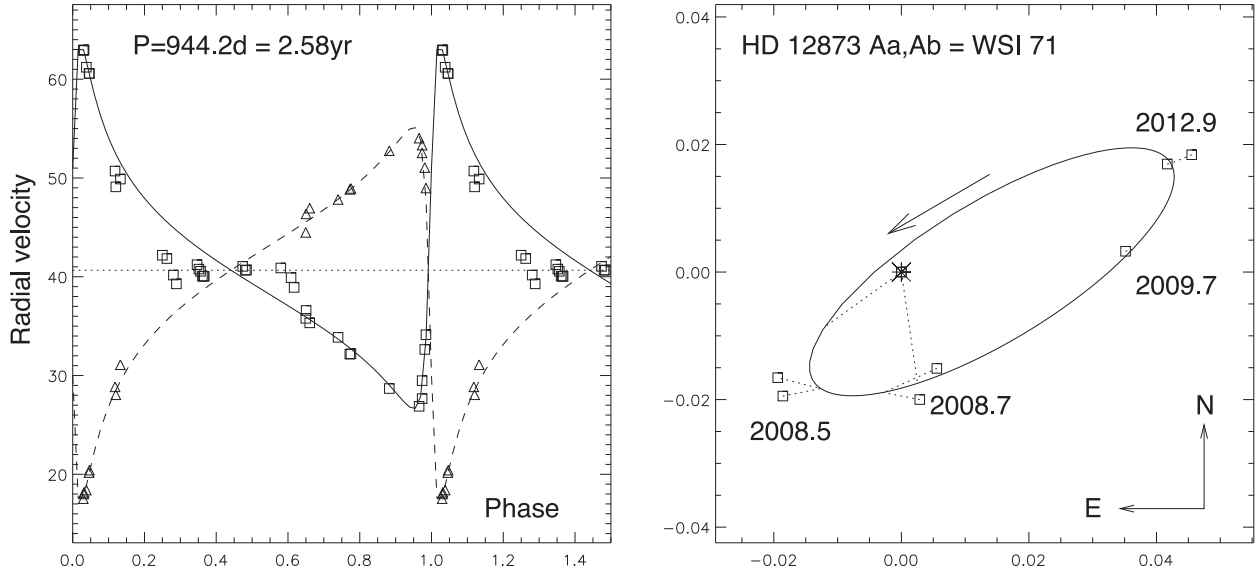| System	P (yr)	T (yr)	e	a (arcsec)	Ω_A (deg)	ω_A (deg)	i (deg)	K_1 (km s^{-1})	K_2 (km s^{-1})	V_0 (km s^{-1})
Aa, Ab	2.582	2010.917	0.769	0.048	127.2	287.9	75.9	18.52	19.10	40.66
	± 0.003	± 0.015	± 0.015	± 0.003	± 4.6	± 1.5	± 4.0	± 0.50	± 0.50	± 0.12
A, B	213	2057	0.45	1.03	140	175	76	–	–	–
	± 213	± 43	± 0.84	± 0.66	± 8	± 85	± 11	–	–	–

Figure 4. Combined orbit of ADS 1652 Aa, Ab. Left: RV curves with Aa plotted as squares and Ab as triangles. The blended RVs (phase 0.2 to 0.6) are ignored. Right: orbit in the sky, with scale in arcseconds. The measurements are connected to the ephemeris positions by dashed lines. The two non-resolutions in 2010 and 2014 are depicted by the dashed lines connected to the primary.
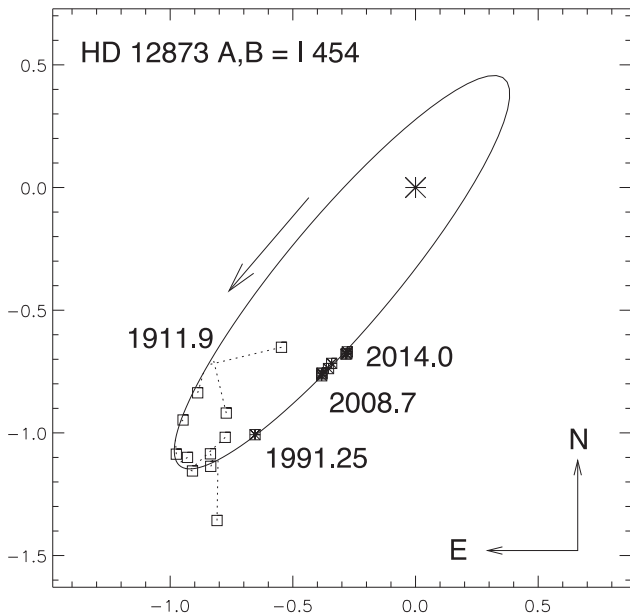

Figure 5. The orbit of A, B = I 454.

Most speckle measurements of Aa, Ab are made at or below the diffraction limit and therefore are rather uncertain, as explained above. This translates to the errors of the semimajor axis and inclination which affect the measurement of stellar masses. The mass

sum computed from the parallax of 22.8 mas and a^3/P^2 is 1.39 M$_\odot$, the spectroscopic mass sum $(M_{Aa} + M_{Ab})\sin^3 i = 1.035\ 10^{-7}(1 - e^2)^{3/2}(K_1 + K_2)^3 P$ corrected for the inclination is 1.46 M$_\odot$. Therefore, the combined orbit of Aa, Ab is consistent with the parallax and gives reasonable (although not very accurate) masses of the components.

4 THE ORBIT OF A, B

The orbital elements of A, B are also listed in Table 4. They differ little from the preliminary (grade 5) orbit by Hartkopf et al. (2012); the difference is caused by the larger weights assigned here to the speckle and *Hipparcos* data, at the detriment of micrometer measurements. Observations of this pair during one century cover only a fraction of the orbit (Fig. 5) and constrain poorly its period and eccentricity, hence the large errors of these elements. On the other hand, the orbital curvature and the inclination are defined quite well. The orbit and parallax of 22.8 mas lead to the mass sum of 2.0 M$_\odot$; the ratio a^3/P^2 that determines the mass is defined much better than the elements P and a themselves (Lucy 2014). As A and B are now approaching, their relative motion will be faster in the coming decades, leading to the improved orbit of A, B. To save the space, we provide the individual measurements of A, B and residuals to the orbit as supplementary data in Table S1, whose format is identical to Table 6.

The speckle measurements of A, B do not define the true ascending node of its orbit without additional RV data. In principle, we can select the correct node from a single measurement of the

Table 5. RVs and residuals of ADS 1652 Aa, Ab.

JD +240 0000	Aa (km s⁻¹) RV	Err	O−C	Ab (km s⁻¹) RV	Err	O−C	In.
499 89.452	50.70	2.42	−1.45	28.85	2.53	0.05	R
499 91.487	49.10	2.57	−2.90	28.05	2.58	−0.90	R
500 03.470	49.89	2.36	−1.27	31.09	2.37	1.27	R
503 24.531	41.05	30.32	1.22	–	–	–	R
503 31.510	40.65	30.32	0.99	–	–	–	R
507 09.534	28.68	0.42	−0.18	52.76	0.35	−0.05	R
510 55.564	42.18	30.77	−3.68	–	–	–	R
510 67.530	41.84	30.33	−3.59	–	–	–	R
510 84.548	40.17	30.37	−4.68	–	–	–	R
510 92.484	39.28	30.40	−5.31	–	–	–	R
514 42.503	35.33	1.37	−0.30	46.94	1.41	1.10	R
532 50.536	40.89	30.38	3.36	–	–	–	R
532 77.492	39.91	30.52	3.03	–	–	–	R
532 85.476	38.92	30.90	2.23	–	–	–	R
536 13.587	26.88	0.66	−0.40	54.03	0.57	−0.41	R
536 21.548	29.48	0.52	0.66	53.32	1.13	0.47	R
536 21.548	27.66	1.05	−1.16	52.54	0.93	−0.31	R
536 28.526	32.64	1.39	0.87	51.05	2.20	1.24	R
536 31.554	34.13	0.51	0.33	48.98	0.75	1.26	R
539 72.584	41.22	30.34	−1.83	–	–	–	R
539 77.589	40.77	30.39	−2.13	–	–	–	R
539 81.571	40.55	30.31	−2.24	–	–	–	R
539 86.546	40.06	30.31	−2.59	–	–	–	R
539 89.544	40.04	30.58	−2.53	–	–	–	R
539 91.563	40.04	30.43	−2.48	–	–	–	R
541 02.524	40.69	30.00	0.96	–	–	–	L
542 57.951	35.79	1.00	−0.19	44.49	1.00	−0.99	L
542 58.929	36.59	1.00	0.64	46.36	1.00	0.86	L
543 42.799	33.87	0.50	0.13	47.82	0.50	0.04	M
543 73.540	32.16	2.37	−0.67	48.84	2.48	0.12	R
543 76.489	32.20	0.36	−0.54	48.94	0.47	0.13	R
546 15.922	62.91	0.50	−0.02	17.53	0.50	−0.15	F
546 16.921	62.97	0.50	0.16	18.01	0.50	0.20	F
546 17.914	62.94	0.50	0.26	18.17	0.50	0.23	F
546 23.908	61.21	0.50	−0.56	18.40	0.50	−0.48	F
546 30.916	60.60	0.50	0.11	20.17	0.50	0.11	F
546 31.911	60.57	0.50	0.11	20.42	0.50	0.19	F

Instruments: R – RVM; L – echelle at the du Pont 100-inch; M – Mike at Magellan Clay; F – fibre echelle at CTIO 1.5 m.

Table 6. Speckle interferometry of ADS 1652 Aa, Ab.

Epoch	θ (deg)	ρ (arcsec)	σ_ρ (arcsec)	(O−C)$_\theta$ (deg)	(O−C)$_\rho$ (arcsec)
2008.5406	136.3	0.027	0.010	−9.0	0.005
2008.5406	140.3	0.025	0.010	−14.8	0.003
2008.7674	188.2	0.020	0.010	16.9	0.001
2008.7727	200.2	0.016	0.010	28.2	−0.003
2009.7558	275.3	0.035	0.005	−0.3	−0.001
2010.9655	–	<0.02	–	(125.6)	(0.015)
2012.9205	292.0	0.049	0.005	0.6	0.002
2012.9233	292.1	0.045	0.002	0.7	−0.002
2014.0457	–	<0.02	–	(198.3)	(0.018)

RV difference between B and the centre of mass of A. In 2008, RV(B)=41.93 km s⁻¹ was measured by fitting three Gaussians to the CCF. This measurement was confirmed by subtracting the spectra of Aa and Ab and correlating the remaining spectrum of B with the solar mask. The RV difference with $V_0 = 40.66$ km s⁻¹ is only $+0.27$ km s⁻¹. The orbit of AB corresponds to $K_1 + K_2 = 6.8$ km s⁻¹

and predicts the RV difference $RV(B) − RV(A) = −1.9$ km s⁻¹ in 2008.5.

Changing the node by 180° would not remove the discrepancy between the small measured RV difference and its larger predicted value, while their signs will match. Taking advantage of poor observational constraints, we found orbital solutions for AB with larger eccentricity that result in a smaller RV difference in 2008.5 and only slightly increase the residuals. However, considering that B can be a binary, we do not attach significance to the measured RV difference and consider that the true node of AB remains indeterminate, so far.

Mutual orientation of orbits in multiple systems informs us on their formation mechanisms. A co-planar and corotating system is expected if it formed by a collapse of an isolated rotating core. On the other hand, dynamical interactions in clusters create multiples with misaligned orbits. The directions of inner and outer angular momenta in triple stars are partially correlated (Sterzik & Tokovinin 2002). However, in 2002, the number of triples where both inner and outer visual orbits were known was only 22 because inner binaries are hard to resolve while outer binaries are too slow. This study adds another system with known inner and outer orbits. The mutual inclination Φ between the two orbits is determined as $\cos\Phi = \cos i_1 \cos i_2 + \sin i_1 \sin i_2 \cos(\Omega_1 − \Omega_2)$. For the selected node of AB, we obtain $\Phi = 12°$, i.e. nearly co-planar orbits, while the alternative choice of $\Omega_{AB} = 320°$ leads to $\Phi = 150°$, or strongly misaligned orbital spins.

5 PHOTOMETRY AND MASSES

The photometry of the stars comprising ADS 1652 is given in Table 7. The combined magnitudes and colours of AB and C are taken from SIMBAD, the individual V magnitudes of the components are then computed using the measured magnitude differences. We adopt $\Delta V_{Aa,Ab} = 0.23$ mag and $\Delta V_{AB} = 2.70$ mag based on all available data.

The 'spectroscopic' magnitude difference is estimated from the ratio of the areas of the Gaussians that approximate the CCF (Table 2) as $\Delta m_{Aa,Ab} = 0.23$ and $\Delta m_{AB} = 2.60$. Here, we assumed that the dip of B has the same FWHM as those of Aa and Ab, not trusting the larger FWHM resulting from the three-component fit. The CCF was computed over the wavelength range 450–650 nm centred on the V band. However, the component B has a lower effective temperature and stronger lines than Aa and Ab, hence in reality $\Delta V(AB) > 2.60$. This spectroscopic estimate agrees with the *Hipparcos* and *Tycho* photometry, $\Delta Hp_{AB} = 2.65$ and $\Delta V_{AB} = 2.75 \pm 0.09$.

The published speckle interferometry measurements of the magnitude difference for the system A, B refer to Aa, B when the triple was resolved and to A, B otherwise. We re-fitted the power spectra by a binary-star model of A, B (ignoring the sub-system) to get more consistent relative photometry of the wide pair. The Δy_{AB} measured on five epochs ranged from 2.55 to 2.83 mag, with the average 2.70 mag and rms scatter of 0.11 mag. Measurements of

Table 7. Photometry of the multiple system ADS 1652.

Parameter	A+B	A	Aa	Ab	B	C
V, mag	8.54	8.62	9.27	9.50	11.32	8.96
$(B − V)$, mag	0.88	–	–	–	–	0.81
$(V − K)$, mag	2.19	–	–	–	–	1.89
$\mathcal{M}(V)$, M$_\odot$	2.37	1.70	0.86	0.84	0.67	0.89
$\mathcal{M}_{orb}$, M$_\odot$	2.03	1.46	0.74	0.72	0.57	0.78

ΔI_{AB} on four epochs average to 2.10 mag with rms scatter of 0.17 mag.

We compare the observed parameters of this system with standard mass–magnitude relations for low-mass main-sequence stars (Henry & McCarthy 1993; Baraffe et al. 1998). The distance modulus is 3.21 mag (parallax 22.8 mas), so the absolute V magnitudes correspond to the masses $\mathcal{M}(V)$ listed in Table 7. They are larger than the masses of Aa and Ab derived from the Aa, Ab orbit, 0.74 and 0.72 $M_\odot$. Adopting the measured masses of Aa and Ab, we find the masses of B and C that match the measured magnitude differences in the V band, as listed in the M_{orb} line of the table. The mass sum of AB is then 2.03 $M_\odot$, matching the orbit of AB.

The measured 'orbital' masses are 14 per cent smaller than the masses derived from the absolute magnitudes. Standard relations predict that stars with such masses should be 1.1 mag fainter than actually observed, and their $V - K$ colour should be redder than measured by $\sim$0.8 mag.

The discrepancy cannot be solved by revising the distance to the system, well constrained by the *Hipparcos* parallaxes of A and C and by the combined orbit. The 'spectroscopic' masses of Aa, Ab would match the standard relation for an orbital inclination of 69° instead of 76°. Although the speckle measurements are not very accurate, they exclude such low inclination. Other orbital elements that influence the spectroscopic masses, P, e, K_1 and K_2, are well defined by the RVs.

We believe that the components of ADS 1652 are indeed brighter and bluer than normal dwarfs of similar mass because they are metal poor. The centre-of-mass RV is $+40.6$ km s^{-1} and the *Hipparcos* astrometry lead to the heliocentric Galactic velocities $[U, V, W]$ $= [-66.4, -71.5, -14.9]$ km s^{-1}. Moderately fast space motion suggests an old age of this system. It does not belong to any known kinematic group. Both stars are slightly metal deficient, [Fe/H] $= -0.37$ and [Fe/H] $= -0.14$ for AB and C, respectively, according to Jenkins et al. (2008), who overlooked however the triple nature of AB. Both components are not chromospherically active, log $R'_{HK} \sim$ -5.1, according to the same authors. The kinematics, metallicity, activity, and rotation, taken together, imply that the multiple system is not young.

6 DISCUSSION

ADS 1652 is a quadruple system composed of main-sequence stars. The 'heaviest' star C of spectral type G8V is single, while the other component of the wide pair is triple and its combined mass exceeds the mass of C. The spectral type of Aa and Ab is G9V, the smallest star B has a mass of 0.6 $M_\odot$ corresponding to the spectral type K5V.

So far, we cannot exclude the existence of additional components. If C were orbited by a low-mass star with a period of a few hundred years, this star would not produce measurable RV variation and would remain unresolved by speckle interferometry owing to its low brightness. Similarly, the component B could be itself a close pair; its six RV observations in 2008 exclude only short-period subsystems, while the mass sum of AB derived from its orbit is not accurate enough to exclude sub-systems in B.

The orbital elements Ω and i of A, B and Aa, Ab are similar, suggesting co-planarity, although this cannot yet be proven observationally. On the other hand, the large eccentricity of Aa, Ab, $e = 0.77$, could be a result of Kozai cycles if the orbits are highly inclined. The multiple system is likely old, hence it should be dynamically stable to survive for several Gyr. The perturbations from the distant companion C should also be small enough, implying

that it never comes too close to AB and its orbit cannot have very high eccentricity. The period of A,C estimated from its projected separation is of the order of 10^5 yr.

Returning to the question posed in the Introduction, we see that the triple component AB has a larger mass and total angular momentum than the single star C. Either the formation of binary companions around C was inhibited, or such companions merged, allowing the star C to accrete all its mass without becoming a binary. The sample of solar-type dwarfs within 67 pc of the Sun (Tokovinin 2014) contains several multiple systems with three-tier hierarchy that bear similarity to ADS 1652. We list two analogues below using compact bracket notation, where each sub-system is characterized by its component's masses and period like $(\mathcal{M}_1, \mathcal{M}_2; P)$. HIP 79607: (((1.15, 1.14; 1.1 d), 1.04; 726 yr), (0.40, 0.13; 52 yr); 0.8 Myr). HIP 103641: (((1.24, 1.05; 112.6 d), 0.70; 400 yr), (0.67, 0.53; 20 yr); 5 Myr). In both multiple systems, the inner 'twin' pairs have short periods, the periods at intermediate level are a few hundred years, and the distant components are themselves close pairs, making these systems quintuple.

The multiple system ADS 1652 merits further study. Speckle interferometry at 8-m telescopes can provide accurate measurements of the inner pair Aa, Ab (barely resolved at 4-m telescopes) to determine its orbit with better accuracy and to solve the mass discrepancy. A similar result can be obtained with long-baseline interferometers in the infrared. Periastrons of Aa, Ab should be monitored with high-resolution spectrographs to improve the accuracy of the orbit and to measure the RV of B, constraining the existence of its sub-systems and fixing the node of the A, B orbit. Accurate RV monitoring of C will help to prove that it is a single star.

The observational story of ADS 1652 is remarkable by the number of telescopes, instruments, and countries involved. Astronomers collected the observations used here for more than a century. Technological progress during this period is reflected in the vastly improved accuracy of the recent measurements. However, it also highlights the value of the old (even inaccurate) data which can't be replaced by modern observations.

REFERENCES

Abt H. A., 1970, ApJS, 19, 387
Aitken R. G., 1932, New General Catalogue of Double Stars. Carnegie Inst. Washington Publ., No. 417, Washington, DC
Baraffe I., Chabrier G., Allard F., Hauschildt P. H., 1998, A&A, 337, 403
Baranne A. et al., 1996, A&AS, 119, 373
Bate M. R., 2012, MNRAS, 419, 3115
Boss L., Roy A. J., 1918, Albany Zone Catalogues for the Epoch 1900. Carnegie Inst. Washington, Washington, DC
Hartkopf W. I., Tokovinin A., Mason B. D., 2012, AJ, 143, 42
Henry T. J., McCarthy D. W., 1993, AJ, 106, 773
Hinkle K., Wallace L., Livingston W., 1995, PASP, 107, 1042
Innes R. T. A., 1912, Transvaal Obs. Circ. 1, 111
Jenkins J. S., Jones H. R. A., Pavlenko Y., Pinfield D. J., Barnes J. R., Lyubchik Y., 2008, A&A, 485, 571
Lucy L., 2014, A&A, 563, 126

Morbey C., 1992, in McAlister H. A., Hartkopf W. I., eds, ASP Conf. Ser., Vol. 32, Complementary Approaches to Double and Multiple Star Research. Astron. Soc. Pac., San Francisco, p. 127

Piskunov N. E., Valenti J. A., 2002, A&A, 385, 1095

Raghavan D. et al., 2010, ApJS, 190, 1 (R10)

Reipurth Bo, Mikkola S., 2012, Nature, 492, 221

Sterzik M., Tokovinin A., 2002, A&A, 384, 1030

Tokovinin A. A., 1987, Astron. Zh., 64, 196 (SvA, 31, 98)

Tokovinin A., 2012, AJ, 144, 56

Tokovinin A., 2014, AJ, 147, 87

Tokovinin A. A., Gorynya N. A., 2001, A&A, 374, 227

Tokovinin A. A., Smekhov M. G., 2002, A&A, 382, 118

Tokovinin A., Cantarutti R., Tighe R., Schurter P., van der Bliek N., Martinez M., Mondaca E., 2010a, PASP, 122, 1483

Tokovinin A., Mason B. D., Hartkopf W. I., 2010b, AJ, 139, 743

Tokovinin A., Mason B. D., Hartkopf W. I., 2014, AJ, 147, 123

SUPPORTING INFORMATION

Additional Supporting Information may be found in the online version of this article:

Table S1. The quadruple system ADS 1652. (http://mnras.oxfordjournals.org/lookup/suppl/doi:10.1093/mnras/stu1394/-/DC1).

Please note: Oxford University Press is not responsible for the content or functionality of any supporting materials supplied by the authors. Any queries (other than missing material) should be directed to the corresponding author for the article.

This paper has been typeset from a TEX/LATEX file prepared by the author.